ACS APPLIED MATERIALS & INTERFACES

Research Article

www.acsami.org

Easy Synthesis of Surface-Tunable Carbon-Encapsulated Magnetic Nanoparticles: Adsorbents for Selective Isolation and Preconcentration of Organic Pollutants

Hongyun Niu,[†] Yixuan Wang,[†,‡] Xiaole Zhang,[†,§] Zhaofu Meng,[‡] and Yaqi Cai*[,†]

[†]State Key Laboratory of Environmental Chemistry and Ecotoxicology of Research Center for Eco-Environmental Sciences, Chinese Academy of Sciences, Beijing 100085, China

[‡]College of Science, Northwest A & F University, Yangling, Shaanxi 712100, China

[§]College of Chemical Engineering and Biological Technology, Hebei Polytechnic University, Tangshan, 063000, Hebei, China

Supporting Information

ABSTRACT: We have prepared core/shell structured carbon-encapsulated magnetic nanoparticles (CMNPs) with a simple method by using inorganic iron salt and glucose solution as precursor substance. The synthetic procedure does not require the use of organic solvents. We have utilized X-ray photoelectron spectroscopy, infrared spectroscopy, X-ray diffraction, and Raman analysis to examine the surface properties of CMNPs prepared at different temperature. The specific surface areas, magnetization and contents of graphitized carbon on carbon shell of CMNPs increase with heat treatment temperature. The obtained CMNPs are used to adsorb or preconcentrate bisphenol A (BPA), 4-n-nonylphenol (4-NP), 4-tert-octylphenol (4-OP), diethyl phthalate (DEP), dipropyl phthalate (DPP), dibutyl phthalate (DBP) dicyclohexyl phthalate (DCHP), dioctyl phthalate (DOP), sulfonamide, tetracyclines, and quinolones antibiotics organic compounds from water samples. The adsorption of analytes is mainly based on $\pi-\pi$ stacking interaction, hydrophobic interaction and hydrogen bonds between analytes and graphitic carbon. As a result, the adsorption or extraction behaviors of CMNPs to analytes are controlled by the content of oxygen-containing species and graphitized carbon on carbon shell of CMNPs. CMNPs prepared at 200 °C have ample oxygen-containing species (80%) on surface and favor the adsorption and extraction of quinolones antibiotics. CMNPs heated at 300−500 °C with the graphitization efficiency of carbon shell lower than 50% exhibit great preconcentration performance to BPA, 4-NP, 4-OP, DBP, DCHP, DOP, tetracyclines, and quinolones antibiotics. CMNPs prepared at 850 °C are highly graphitized (80%) and have strong adsorption affinity to all model analytes; however, they can quantitatively extract only highly polar sulfonamide antibiotics and moderately polar DEP, DPP because of hard desorption of other model analytes. We suggest that the appropriate adsorbent to certain organic contaminants can be obtained with this technique just by tuning the heat temperature without any post-treatment.

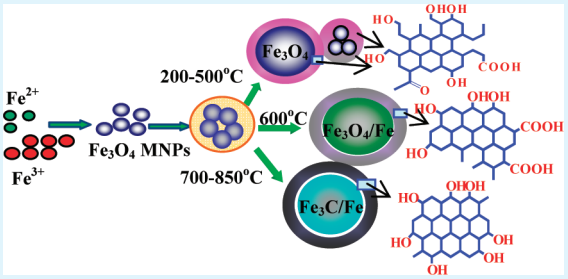

KEYWORDS: *surface-tunable carbon-encapsulated magnetic nanoparticles, graphitized carbon, oxygen-containing species, solid-phase extraction, adsorption*

1. INTRODUCTION

Analysis of organic pollutants often requires preconcentration of the analytes from large volumes of solutions. Solid-phase extraction (SPE) has become a well-established sample preparation method to preconcentrate desired components from sample matrix. When applying SPE method, the selection of the most appropriate adsorbent is of vital importance to allow an efficient isolation/preconcentration of the analytes and ensure the sensitivity, selectivity and precision of the results.[1] Nanomaterials should be the ideal candidate for SPE adsorbents because of their large surface areas and short diffusion route, which may result in high extraction efficiency and rapid extraction kinetics. To avoid the disadvantages of nanomaterials such as high backpressure and long sample loading time when they are packed into cartridge to extract pollutants, magnetic solid-phase extraction, a novel SPE method, has been developed based on the use of magnetic nanoparticles.[2−13] The magnetic adsorbents are usually well devised with core/shell structure. The inner core is composed of metal oxides especially Fe_3O_4 nanoparticles. The coat includes functionalized metal oxide,[3,4] organsilane (bearing C_{18}, or aminopropyl groups),[2,5,6] polymer,[7,8] biomass,[5,6,9] hemimicelles/admicelles of ionic surfactant or alkyl carboxylates,[10−12] and so on. However, these coats still can not prevent the agglomeration and oxidation of nanoparticles in certain conditions (such as acid solution). Carbon-based materials, including graphitized carbon black, carbon nanotubes (CNTs) and fullerenes, have strong adsorption affinity to a

Received: September 28, 2011
Accepted: December 7, 2011
Published: December 7, 2011

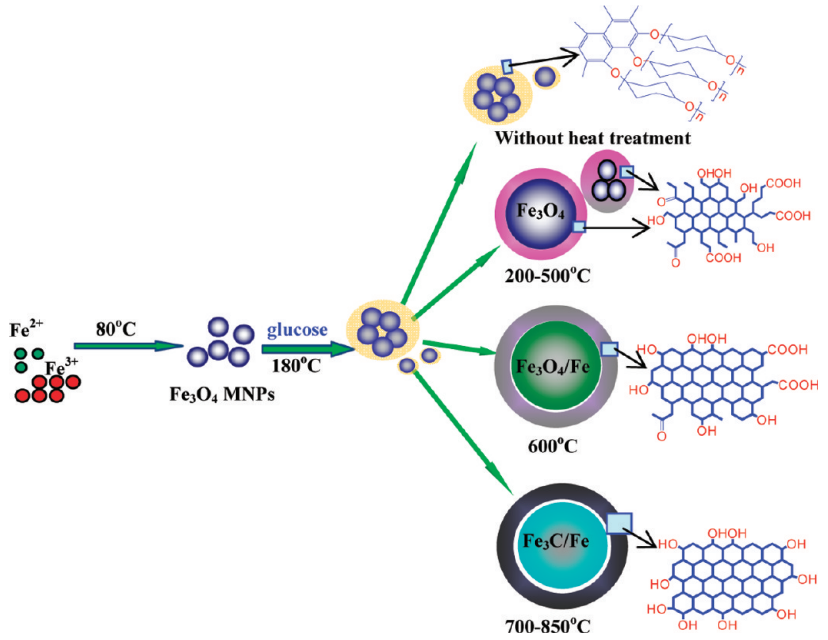

Figure 1. Schematic diagram of preparation of CMNPs with different surface propriety.

wide variety of organic species and effectiveness over a broad pH range, which makes them excellent material for SPE.[14] Therefore, carbon seems to be the most desired material for encapsulation.

In recent years, carbon-encapsulated metal nanoparticles (CMNPs) have attracted great interest all over the world. This material is composed of metallic core and carbon coat. The crystallinity of the coat is of graphitic nature and similar to carbon nanotubes.[15] It can be expected that CMNPs display comparable SPE behaviors to CNTs to organic compounds. By far, the research works about CMNPs are mainly focused on their synthesis and structure. CMNPs have been prepared with laser assisted irradiation,[16] arc discharge,[17] thermal plasma,[18] microwave heating,[19] spray pysolysis,[20] explosion,[21] and chemical vapor condensation[22] methods. However, most of these methods involve relatively harsh reaction conditions that typically lead to operational complexity, high cost, or difficulties in terms of practical applications. Song group have synthesized CMNPs by using aromatic heavy oil or phenolic resin as carbon source and ferrocene as metal source via cocarbonization at 420−510 °C under pressure.[23−26] Geng et al. reported a direct salt-conversion approach for large-scale synthesis of CMNPs by pyrolysis of iron stearate under argon.[27] The two methods are simple but demand toxic reagents.

Recently, a new kind of metal/carbon hybrid has been synthesized with hydrothermal method by heating the mixture of Fe_3O_4 nanoparticles or noble metal salts and glucose or soluble starch solution at 160−200 °C.[28−31] The carbon coat is formed resulting from the aromatization and carbonization of glucose and remains plenty of oxy-containing groups.[28,32] In our previous work, we have used the carbon coated Fe_3O_4 nanoparticles prepared with this method as SPE adsorbent to extract polycyclic aromatic hydrocarbons (PAHs) from water samples.[29] As a result, this material showed strong extraction ability to PAHs. Because the carbon coat is poorly graphitized and highly hydrophilic,[28−32] the low extraction performance of this adsorbent can be expected to organic compounds with medium and high polarity. It is necessary to enhance the graphitization degree of the carbon coat.

Herein, we establish a simple approach to synthesize CMNPs by first introducing amorphous carbon coat on Fe_3O_4 surface with hydrothermal method and then heating the as-prepared nanoparticles under 200−850 °C in a N_2 atmosphere. The carbon shell will be graphitized under heat catalyzing by the Fe_3O_4 core. This approach is much simpler when compared to other synthetic methods for CMNPs. The synthetic procedure does not require the use of organic solvents or toxic reagents. The method has the potential for scalable synthesis of CMNPs. Furthermore, the surface composition of CMNPs is tunable just by changing the heat temperature. Therefore, the versatility and selectivity of this material can be achieved during its preparation in order to favor interaction with particular molecules without any post-treatment.

2. EXPERIMENTAL SECTION

2.1. Reagents. All reagents used in the experiment were of analytical reagent grade and used without further purification. Diethyl phthalate (DEP), dipropyl phthalate (DPP), dibutyl phthalate (DBP), dicyclohexyl phthalate (DCHP), dioctyl phthalate (DOP), bisphenol A (BPA), and sulfamethazine (SMT), chlorotetracycline hydrochloride (CTC), and tetracycline (TTC) were supplied by Acros Organics (Morris Plains, NJ, USA). Ciprofloxacin (CIF) was from Sigma-Aldrich Co. (St. Louis, MO, USA). Norfloxacin (NOF) was purchased from Toronto Research Chemicals Inc. (North York, ON Canada). 4-N-Nonylphenol (4-NP), 4-tert-octylphenol (4-OP), sulfathiazole (STL), and sulfapyridine (SP) were obtained from Tokyo Kasei Kogyo Co. Ltd. (Tokyo, Japan). Standard stock solutions (phthalate esters and alkyl phenols 500 mg L^{-1}; antibiotics 200 mg L^{-1}) of each compound were prepared in methanol. The mixture of phthalate esters group (50 mg L^{-1} each analyte), alkyl phenols group (50 mg L^{-1} each analyte), sulfonamide antibiotics group (20 mg L^{-1} each analyte), and mixture of tetracyclines and quinolones antibiotics (20 mg L^{-1} each analyte) were prepared by diluting the standard solution with methanol, respectively. The standard stock solutions of phthalate esters and alkyl phenols were stored at 4 °C, and the solutions of antibiotics were kept at −18 °C. Working solutions were prepared daily by appropriate dilution of the stock solutions with ultrapure water. Ferric chloride ($FeCl_3{\cdot}4H_2O$), ferrous chloride ($FeCl_2{\cdot}6H_2O$) and glucose were purchased from Beijing Chemicals Corporation (Beijing, China). HPLC-grade acetonitrile and methanol was obtained

dx.doi.org/10.1021/am201336n | ACS Appl. Mater. Interfaces 2012, 4, 286−295

Table 1. HPLC Analysis Information of All the Model Analytes

analytes	eluent	gradient elution	wavelength
phthalate esters	A: acetonitrile	0−15 min B 40%,	226 nm
	B: water/acetonitrile (50:50)	15−25 min B 40−100%	
		25−35 min B 100%	
		35−36 min B 100−40%	
		36−40 min B 40%	
alkyl phenols	A: acetonitrile	0−3 min B 100%	Ex. 220 nm, Em. 315 nm
	B: water/acetonitrile (50:50)	3−15 min B 100−0%	
		15−17 min B 0%	
		17−19 min B 0−100%	
		19−23 min B 100%	
sulfonamide compounds	A: water (pH 3.0, adjusted by 0.2 M KH_2PO_4 and 0.2 M H_3PO_4)	0−10 min B 12%	260 nm
		10−20 min B 12−40%	
		20−25 min B 40%	
	B: water/acetonitrile (20:80)	25−30 min B 40−12%	
		30−35 min B 12%	
tetracycline, quinolones antibiotics	A: 6 mmol L^{-1} oxalic acid solution/acetonitrile (95:5)	0−7 min B 0−25%	268 nm
		7−12 min B 25%	
	B: 6 mmol L^{-1} oxalic acid solution/methanol/acetonitrile (90:3:7)	12−12.5 min B 0%	
		12.5−20 min B 0%	

Table 2. Specific Surface Area, Element Composition, And Magnetic Characteristic of CMNPs

			element composition (%)				
adsorbent	ΔW (%)[a]	SSA (m^2/g)[b]	C	O	Fe	saturation magnetization (emu/g)	coercivity (Oe)
untreated CMNPs		54.1	65.4	32.8	1.8	24.4	2.64
CMNPs (200)	5.82	60.4	67.4	29.9	2.7	22.5	2.68
CMNPs (300)	8.64	79.0	71.5	26.8	1.8	25.6	2.24
CMNPs (400)	22.1	103	71.5	24.9	3.4	29.9	3.50
CMNPs (500)	40	207	73.4	23.4	3.2	33.8	6.64
CMNPs (600)	45.5	239	78.7	19.1	2.2	82.6	366
CMNPs (700)	48	202	79.7	16.4	3.9	102	322
CMNPs (850)	50.8	134	80.6	14.2	4.2	123	131

[a]Weight loss of CMNPs during preparation. [b]Specific surface areas.

from Fisher Scientific Corporation (Fair Lawn, NJ, USA). Ultrapure water was prepared by using Milli-Q water purification system (Bedford, MA, USA).

2.2. Preparation of Carbon-Encapsulated Magnetic Nanoparticles. Fe_3O_4 nanoparticles (Fe_3O_4 NPs) were prepared by the chemical coprecipitation method. Briefly, 5.2 g of $FeCl_3{\cdot}4H_2O$ and 2.0 g of $FeCl_2{\cdot}6H_2O$ were dissolved in 100 mL of water and heated to 90 °C under N_2, and then 10 mL of ammonium hydroxide (25%) was added into the solution. The mixture was stirred at 90 °C for 30 min. The produced Fe_3O_4 NPs were washed with ultrapure water to neutral. Then 0.4 g of the Fe_3O_4 was dispersed into 80 mL glucose solution (0.5 M). The mixture was transferred in a PTFE-lined autoclave, and heated for 4 h at 180 °C. After reaction, the carbon-encapsulated magnetic nanoparticles (labeled as untreated CMNPs) were washed with ultrapure water and ethanol several times, and then freeze-dried. The as-prepared untreated CMNPs were heated to 200−850 °C with a heat rate of 2 °C min^{-1} and left at the target temperature for 4 h under the protection of N_2. The resulting nanoparticles were washed with ultrapure water and ethanol subsequently and labeled as CMNPs (x) (x = 200, 300, 400, 500, 600, 700, and 850) according to the heat treatment temperature. Illustration of the preparation procedure is shown in Figure 1.

2.3. Characterization of CMNPs. The morphology and particle size of the CMNPs were studied by using a transmission electron microscope (TEM) of H-7500 (Hitachi, Japan) operating at 80 kV accelerated voltage. The specific surface areas of CMNPs were determined by the BET method with N_2 gas (ASAP2000 V3.01A; Micromeritics, Norcross, GA). The crystal phase was investigated by a PANalytical X'pert Pro diffractometer. Magnetic property was analyzed using a vibrating sample magnetometer (VSM, LDJ9600). To detect the composition and chemical state of elements on CMNPs surface, some selected samples were freeze-dried for further analysis using X-ray photoelectron spectroscopy (XPS) collected on an ESCALab-200i-XL spectrometer with monochromatic Al Kα radiation (1486.6 eV). FTIR spectra were taken in KBr pressed pellets on a NEXUS 670 Infrared Fourier Transform Spectrometer (Nicolet Thermo, USA). Raman analysis was carried out using a Microscopic Confocal Renishaw Raman Spectrometer (RM2000). Two laser lines were used to excite the sample, 514 nm (green laser) and 632 nm (red laser).

2.4. SPE Procedure. Fifty milligrams of CMNPs were rinsed and activated with 5 mL of methanol, then dispersed into 500 mL of water sample in a 600 mL glass beaker containing trace level of target compounds. The mixture was sonicated for 1 min and placed for 30 min. Subsequently, the beaker was placed on the top of an Nd−Fe−B strong magnet with a size of 150 × 130 × 50 mm^3 and the nanoparticles were isolated from solution. After about 10 min, the solution became limpid and the supernatant was decanted. Finally, analytes were eluted from the recovered particles with an appropriate eluent. The eluate was evaporated to about 0.2−0.3 mL with a stream of nitrogen at 50 °C and then diluted to 0.5 mL with acetonitrile, and 20 μL of this solution was injected into the HPLC system for analysis.

2.5. Batch Experiments. Batch experiments were performed in 50 mL of polyethylene bottles. The final aqueous volume in each bottle was 30 mL. The ionic strength was controlled to 10 mmol L^{-1} with 1 mol L^{-1} NaCl solution. The dosage of CMNPs was 100 mg L^{-1}. Adsorption isotherm studies were conducted with initial antibiotics concentrations ranging in 0.5−20 mg L^{-1} at neutral pH in ultrapure

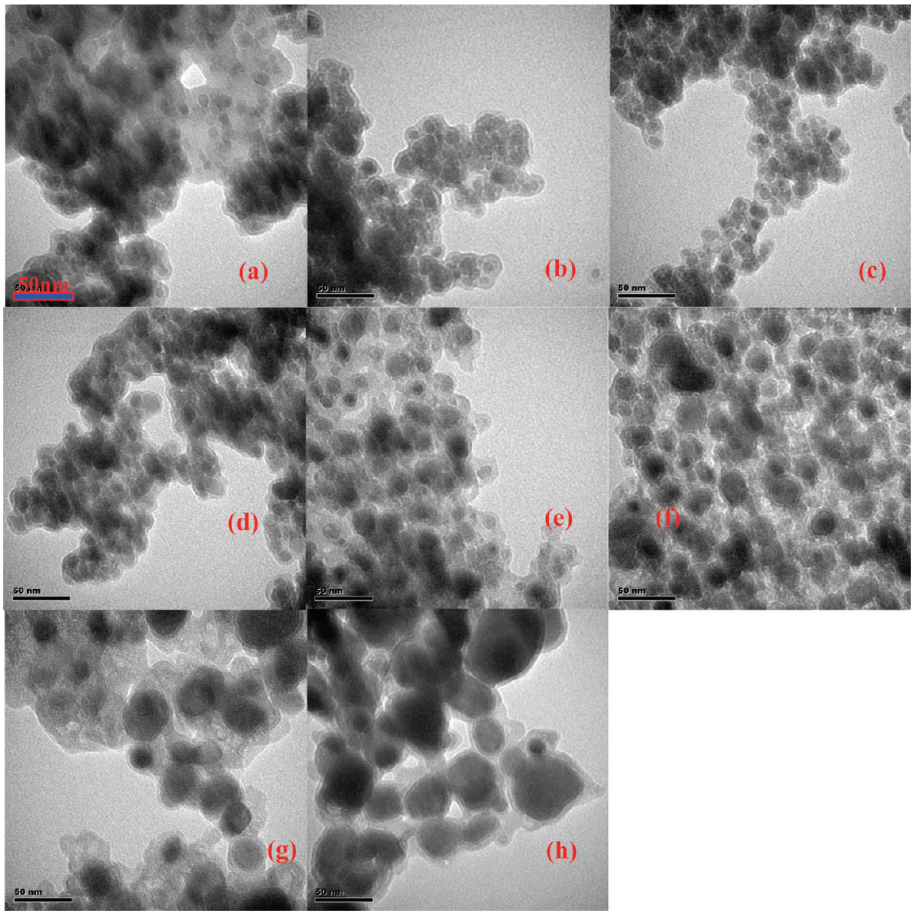

Figure 2. TEM images of CMNPs prepared at different temperature (a) untreated CMNPs, (b) CMNPs (200), (c) CMNPs (300), (d) CMNPs (400), (e) CMNPs (500), (f) CMNPs (600), (g) CMNPs (700), (h) CMNPs (850); the scale bar in all the images represents 50 nm.

water. After mixing for 24 h at 25 °C in a shaken water bath (200 rpm), the mixture was centrifuged at 10 000 rpm for 10 min. The supernatant aqueous solution was used for the analysis of model compounds.

2.6. HPLC Analysis. All the analytes were separated and quantified by using a HPLC system (DIONEX, USA). The HPLC equipment included a DIONEX P680 HPLC pump, a thermostatted column compartment TCC-100, a DIONEX RF 2000 fluorescence detector (FLD) for BPA, 4-NP, and 4-OP, and a PDA-100 photodiode array detector for other compounds. The separations were conducted on a Diamonsil C_{18} column (250 × 4.6 mm; particle size, 5 μm) (Dikma Technologies, Beijing, China). The mobile phase, gradient elution and detection wavelength for phthalate esters, alkyl phenols (BPA, 4-NP, and 4-OP), sulfonamide compounds, and mixture of tetracycline and quinolones antibiotics were listed in Table 1. The flow rate for all analytes was 1 mL min^{-1}.

3. RESULTS AND DISCUSSION

3.1. Characterization of CMNPs. It has been reported that the iron nanoparticles has a very high catalytic activity and greatly promotes the graphitization during heat treatment. At the same time, the iron oxide (Fe_3O_4) is reduced by carbon (equation: $Fe_3O_4 + 2C = 3Fe+2CO_2$).[24] The weight loss of CMNPs before and after heat treatment is listed in Table 2. As the temperature changes from 200 to 850 °C, the weight loss is increased from 5.8 to 51%. The first and second sharp increase of weight loss is observed at 400 and 500 °C, respectively, which indicates that graphitization efficiencies are clearly enhanced at >500 °C. In the TEM image of untreated CMNPs (Figure 2a), several Fe_3O_4 NPs (about 10 nm in diameter), rather than single nanoparticle, are imbedded in carbon shell. The actual particle size of this material is large and hard to define in TEM image. With the increase of heat temperature, the numbers of Fe_3O_4 NPs in carbon coat are decreased gradually, leading to the decrease of the actual particle size of CMNPs (Figure 2b-d). As the heat temperature is higher than 500 °C, the typical core/shell structure of CMNPs is discerned and CMNPs with single iron core exist. The particle sizes of CMNPs (500) are about 30 nm, and the sizes of CMNPs (600), CMNPs (700) and CMNPs (850) are in the range of 20−40, 30−50, and 40−100 nm, respectively (Figure 2e−h). The specific surface area (SSA) of untreated CMNPs is 54 m^2 g^{-1}. The heat treatment enhances the SSA of CMNPs (Table 2). The highest SSA value is obtained as the temperature is up to 600 °C (240 m^2 g^{-1}); further increase of temperature leads to decreased SSA (134−202 m^2 g^{-1}). The large SSA of CMNPs prepared at high temperature might suggest that there are pores in the graphitized carbon shell with a higher graphitization degree.[33]

The crystal phases of CMNPs are investigated by XRD analysis. As shown in Figure 3a, the crystalline of untreated CMNPs and CMNPs prepared at 200−500 °C matches well with that of cubic crystalline magnetite.[30] In XRD pattern of CMNPs (600), the new peaks appearing at 2θ = 44.7° and 65.0° can be ascribed to the (110) and (200) reflections of α-Fe, respectively,[23,26] suggesting that the metal core encapsulated in the carbon shells is the mixture of Fe_3O_4 and α-Fe. For CMNPs (700) and CMNPs (850), the typical diffractions

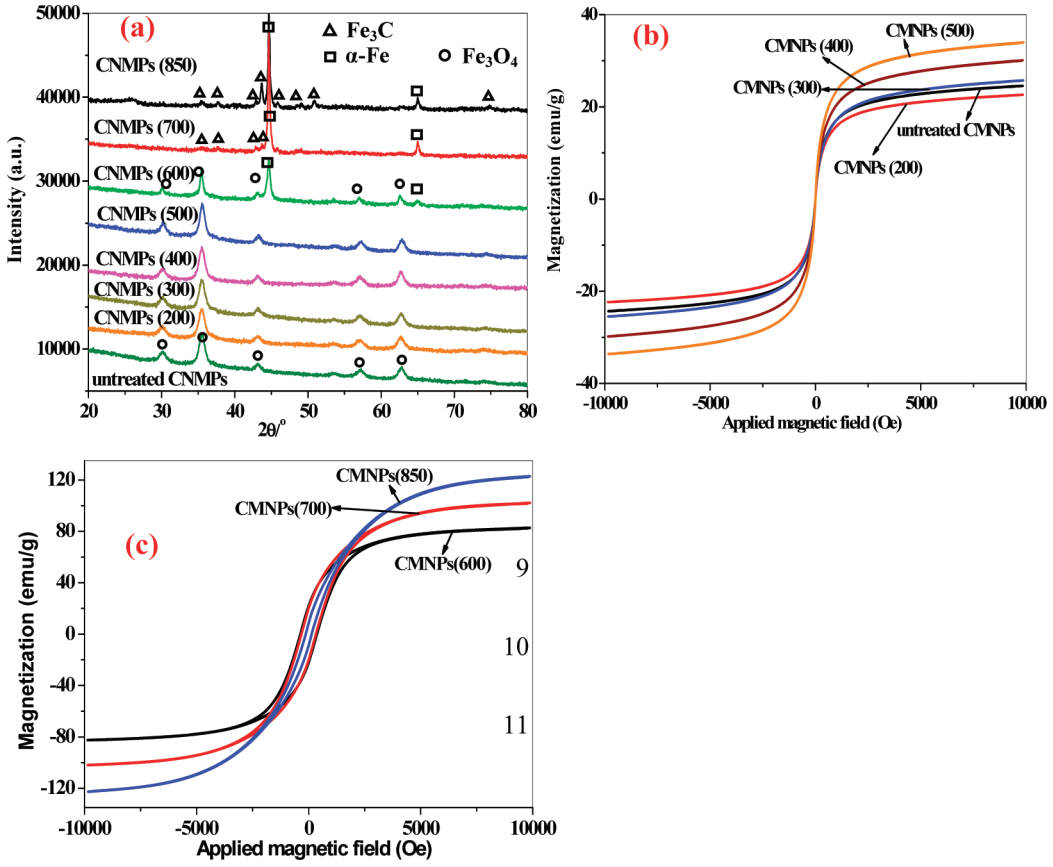

Figure 3. (a) XRD patterns of all the CMNPs, VSM magnetization curves of (b) untreated CMNPs and CMNPs prepared at 200−500 °C and (c) CMNPs obtained at 600−850 °C.

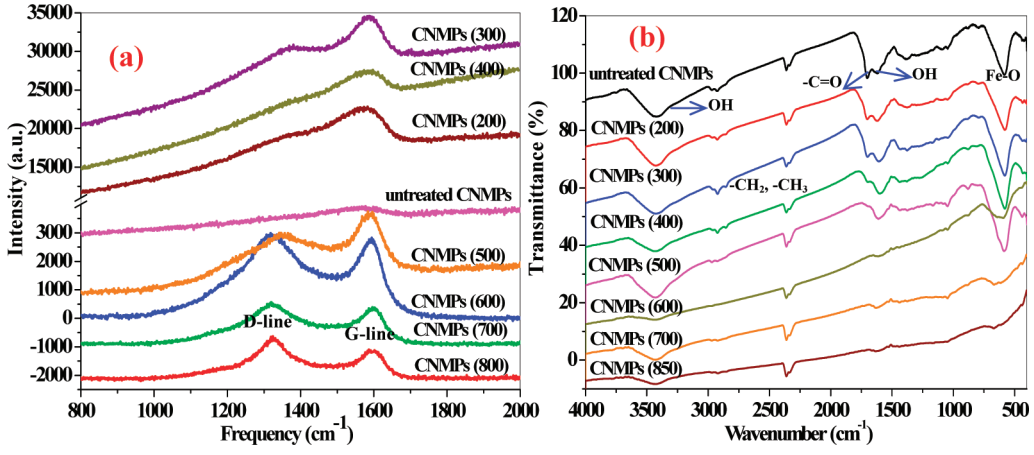

Figure 4. (a) Raman spectra and (b) FTIR spectra of all the CMNPs.

peaks for Fe_3O_4 disappear and small amounts of an iron carbide (Fe_3C) phase, with diffraction peaks at 35.6, 37.6, 42.8, 43.6, 45.9, 49.1, 50.9, and 78.3° appear in the two samples.[23,27] Then the CMNPs (700) and CMNPs (850) samples are carbon-encapsulated metallic α-Fe and iron carbide (Fe_3C). The appearance of iron carbide is indicative of a recrystallization process (dissolution−precipitation) of the carbon material during carbothermal reaction. The increased particle size in Figure 2 at higher temperature is possibly caused by the dissolution of carbon species into iron nanoparticles.[24,25]

Magnetic hysteresis loops measured at room temperature for all the CMNPs are shown in Figure 3b, 3c. In the VSM magnetization curves of untreated CMNPs and CMNPs prepared at 200−500 °C, there is no hysteresis, and the remanence and coercivity is negligible, indicating the superparamagnetism of these nanomaterials (Figure 3b). Their saturation magnetization is ranged in 20−35 emu/g (Table 2). For CMNPs prepared at 600−850 °C, clear hysteresis is observed (Figure 3c), and the coercivity is larger than 130 Oe, which reflect the ferromagnetic characteristic of these nanoparticles. The saturation magnetization of CMNPs (600), CMNPs (700) and CMNPs (850) increase greatly and range in 83−123 emu/g (Table 2). The magnetic characteristic of these CMNPs are agreement with their crystal phases.

dx.doi.org/10.1021/am201336n | ACS Appl. Mater. Interfaces 2012, 4, 286−295

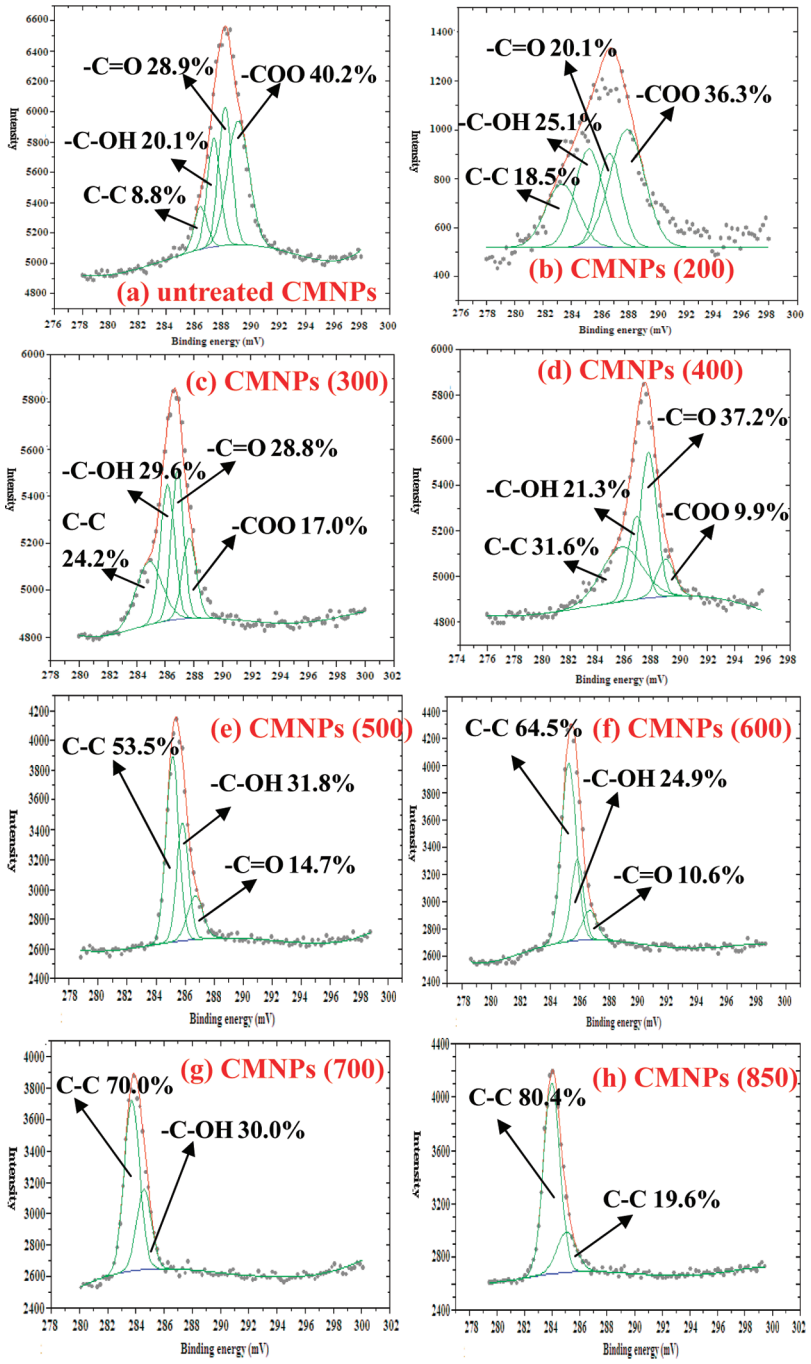

Figure 5. Peak fitting of C1s spectra of CMNPs and the corresponding content of each C species: (a) untreated CMNPs, (b) CMNPs (200), (c) CMNPs (300), (d) CMNPs (400), (e) CMNPs (500), (f) CMNPs (600), (g) CMNPs (700), (h) CMNPs (850).

Raman spectroscopy is a key tool to indentify disorder in sp^2 network of different carbon structures. The Raman spectrum of crystalline graphite is marked by the presence of two peaks centered at 1580 (G-line) and 1350 cm^{-1} (D-line), attributing to in-plane vibrations of crystalline graphite and disordered amorphous carbon, respectively.[34] In the spectra of untreated CMNPs and samples prepared at 200−400 °C, the G-line and D-line cannot be completely defined, which indicates the disordered graphite characteristic of carbon shell on these materials (Figure 4a). In contrast, both the G-line and D-line are discerned in the spectra of CMNPs treated at 500−850 °C, and the peaks become sharp with the increase of heat temperature. This suggests that the carbon shell is graphitized efficiently catalyzed by the Fe_3O_4 core when heat temperature is higher than 500 °C. However, the crystallinity of carbon shell on all CMNPs is poorer than that of CNTs since the low ratio of G-line to D-line intensity.[34]

The surface property of CMNPs is investigated with IR analysis. In the FTIR spectrum of untreated CMNPs, the strong peak at 580 cm^{-1} is related to the Fe−O group (Figure 4b). The peaks at 1620 and 3425 cm^{-1} are corresponding to the surface-sorbed water and hydroxyl groups. The adsorption peaks at 1380, 2920, and 2956 cm^{-1} are ascribed to the bending vibration or stretching vibration of $-CH_2$ and $-CH_3$ species. The peaks around 1700 cm^{-1} can be assigned to the -C═O stretching vibrations from ketones or carboxyl groups. The

dx.doi.org/10.1021/am201336n | ACS Appl. Mater. Interfaces 2012, 4, 286−295

intensities of the adsorption peaks for Fe−O, hydroxyl groups, and $-CH_2$ and $-CH_3$ species are decreased significantly as the heat temperature rises to 600 °C. The peak intensity for -C═O bond is weakened with the increase of treatment temperature, and absent when the temperature is higher than 600 °C. The absence of −C═O bond on CMNPs (600) maybe caused by its low content on its surface. These results clearly show that the surface properties of CMNPs prepared at 600−850 °C are quite different with those of other CMNPs.

The element composition and their atom contents on the surface of CMNPs are analyzed with XPS. Since XPS mainly reveals the information of the surface with a depth of 0.1−10 nm,[29] the Fe contents are lower than 5% on the surface of all CMNPs. With the increase of heat temperature, the C contents increase from 65% to 81%, while the O contents decrease from 33% to 14% (Table 2). The C 1s peak deconvolution of all the adsorbents are shown in Figure 5. Compared with the C 1s lines of untreated CMNPs, CMNPs (200) and CMNPs (300), the C1s peaks of CMNPs prepared at 300−850 °C are found to shift to lower binding energies. The shift degree of CMNPs (700) and CMNPs (850) is larger than those of CMNPs heated at 300−600 °C. In XPS spectra, the chemical shifts in the core levels provide information on the oxidation state of different species. The spectra of C 1s of all the CMNPs adsorbents are fitted using a 50:50 Gian:Lorentzian peak shape. In the spectra of untreated CMNPs and CMNPs prepared at 200−400 °C, the C 1s peak is composed of overlapped peaks of C−C (284.5 eV), −C−O (286.3 eV), −C═O (287.9 eV), and −COO (289.9 eV).[35] On the surface of untreated CMNPs and CMNPs (200), −COO group is the most abundant (36−40%) species, and the content of C−C, representing graphitic carbon, is less than 19%. The percent of −COO group decreases rapidly with the increase of heat temperature and disappears as the temperature is higher than 400 °C. On the surface of CMNPs (500) and CMNPs (600), the content of C−C and −C═O group is >50% and <15%, respectively. There is only C−C and −C−O species left on the surface of CMNPs (700) and CMNPs (850), and the percent of −C−O group is ranged in 20−30%. These suggest that the graphitization efficiency of carbon shell on CMNPs is enhanced with the increase of heat temperature. However, there still remain a rather high number of O-functional groups on CMNPs surface, which is agreement with the results of Raman spectroscopy.

The above-mentioned results indicate that CMNPs with core/shell structure have been successfully synthesized by using this method. The synthetic procedure is simple and does not involve the toxic chemicals. Most importantly, the surface characteristic of CMNPs is tunable just by changing the graphitization degree of carbon and controlling the amount of oxygen-containing species on carbon shell under different heat treatment temperature.

3.2. Extraction Performance of CMNPs to Organic Pollutants with Weak or Medium Polarity. All CMNPs (50 mg) are used as adsorbents to extract trace organic pollutants with different polarity from 500 mL of water samples. The model compounds include five phthalate esters, BPA, 4-NP, and 4-OP. The target compounds can be desorbed with acetonitrile.

The extraction efficiency of these compounds is dependent on the surface property of CMNPs and the polarity of compounds (Figure 6). Among the selected phthalate esters, DOP is the most hydrophobic compound (lgKow = 8.3).[36] The recoveries of DOP are higher than 80% as CMNPs (200) and

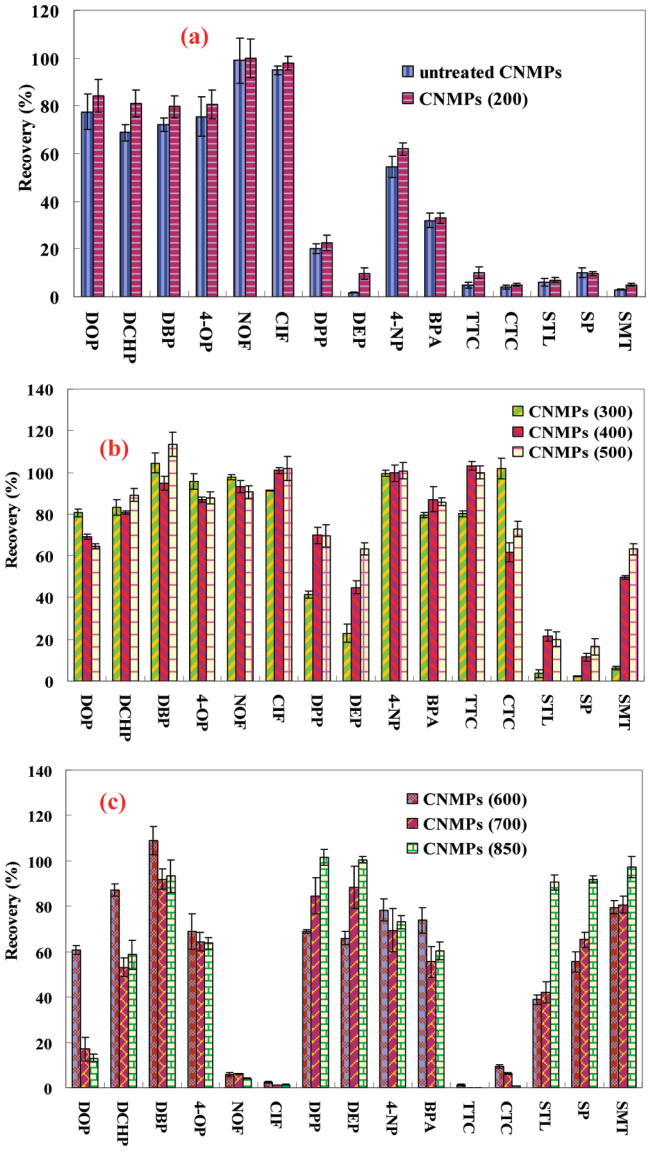

Figure 6. Extraction efficiency of target compounds using (a) untreated CMNPs and CMNPs (200); (b) CMNPs (300), CMNPs (400) and CMNPs (500); and (c) CMNPs (600), CMNPs (700) and CMNPs (850) as SPE adsorbents.

CMNPs (300) are used as SPE adsorbent, and then decrease remarkably with the rising temperature of adsorbents during their preparation. DCHP (lgKow = 6.02)[36] is quantitatively recovered by CMNPs prepared at 200−600 °C. For DBP (lgKow = 4.63),[36] the recoveries are higher than 90% on the adsorbent of CMNPs obtained at 300−850 °C. The extraction efficiency of DEP and DPP (lgKow = 2.51 and 3.27, respectively)[36] with medium-polarity increase with the graphitization of CMNPs. Satisfactory recoveries of the two compounds are obtained on CMNPs (700) and CMNPs (850). The best extraction performance of BPA, 4-NP, and 4-OP (lgKow = 3.41, 4.12 and 4.48, respectively)[37,38] are achieved on CMNPs prepared at 300−500 °C. Generally the extraction performances of CMNPs prepared at 300−500 °C to these compounds are similar with that of carbon nanotubes (recoveries ranging in 90−100% extracted from 500 mL of water samples).[39,40]

dx.doi.org/10.1021/am201336n | ACS Appl. Mater. Interfaces 2012, 4, 286−295

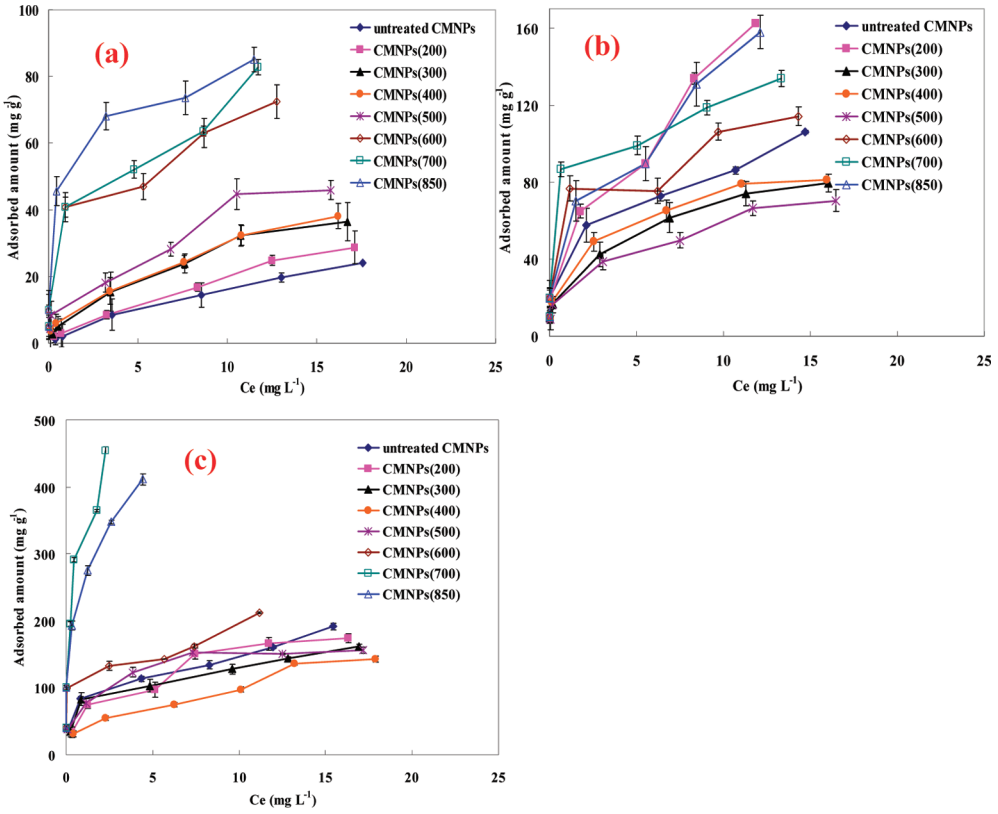

Figure 7. Adsorption isotherms of (a) SMT, (b) NOF, and (c) CTC on all the CMNPs at 25 °C in neutral solution.

The interaction mechanisms between organic chemicals and CNTs have been explained as hydrophobic interactions, $\pi-\pi$ stacking, electrostatic interactions, and hydrogen bonds.[41] Similar to CNTs, the adsorption mechanisms of organic compounds with weak- and medium-polarity on CMNPs should involve $\pi-\pi$ stacking and hydrophobic interaction. Therefore, the increased graphitic carbon content on CMNPs surface is favorable for the retention of these targets. But too strong adsorption always prevents desorption of compounds from CMNPs surface, which leads to low recoveries of these target compounds on CMNPs prepared at 600−850 °C, except DEP, DPP, and DBP.

3.3. Extraction Performance of CMNPs to Antibiotics.

Three sulfonamide antibiotics (sulfamethazine SMT, sulfathiazole STL, sulfapyridine SP), two tetracycline antibiotics (chlortetracycline CTC, tetracycline TTC), and two quinolones (norfloxacin NOF, and ciprofloxacin CIF) are used as model compounds. The extraction efficiency of CMNPs to these amphoteric compounds is not affected by solution pH, which may be explained by the fact that the concentrations of analytes are very low and the amounts of adsorbed analytes are far below their adsorption capacity on CMNPs. The adsorbed antibiotics are hard to be desorbed with acetonitrile or methanol solvent. Oxalic acid solution is required to add to acetonitrile solvent. The optimal eluent is composed of 30% 50 mM oxalic acid solution and 70% acetonitrile.

Figure 6 shows that the three types of antibiotics exhibit different extraction behaviors on these CMNPs adsorbents. The recoveries of SMT, STL, and SP are low when they are extracted by untreated CMNPs and CMNPs prepared at 200−500 °C. Their recoveries increase abruptly on CMNPs (600), CMNPs (700), and CMNPs (850). But the highest and quantitative recoveries of sulfonamides compounds are only achieved on CMNPs (850). The trends for extraction efficiency of the quinolones on CMNPs are just opposite to those of sulfonamides compounds. NOF and CIF can be recovered quantitatively (>90%) from 500 mL water solution as untreated CMNPs and CMNPs prepared at 200−500 °C are used as adsorbents. However, sharp decrease of the recoveries of the quinolones compounds (<10%) are observed on CMNPs (600), CMNPs (700) and CMNPs (850). For CTC and TTC, best recoveries are achieved by using CMNPs (300), CMNPs (400) and CMNPs (500) as SPE adsorbents; but they are hardly recovered (<10%) from solution when they are enriched by untreated CMNPs, CMNPs (200), and CMNPs prepared at 600−800 °C. In general, the extraction tendencies of sulfonamides on these CMNPs resemble those of diethyl-phthalate, dipropyl-phthalat with medium-polarity. Tetracycline and quinolones antibiotics display similar enrichment effects to those of analytes with weak polarity. The extraction efficiencies of these CMNPs to tetracycline and quinolones antibiotics are comparable with those of hydrophilic−lipophilic balance (HLB) adsorbents (83−94%).[42,43]

3.4. Adsorption Behavior of Antibiotics on CMNPs.

To elucidate the extraction behaviors of three types of antibiotics on CMNPs adsorbents, batch experiments are conducted with SMT, NOF, and CTC as model compounds. Langmuir and Freundlich equations are used in the analysis of isotherms of the antibiotics on CMNPs adsorbents. Langmuir isotherm is mainly applied to monolayer adsorption on perfectly smooth and homogeneous surface, whereas Freundlich isotherm is widely employed for adsorption surfaces with nonuniform energy distribution.

dx.doi.org/10.1021/am201336n | ACS Appl. Mater. Interfaces 2012, 4, 286−295

The linearized Langmuir isotherm is given as

$$\frac{C_e}{q_e} = \frac{1}{q_{max}K_L} + \frac{C_e}{q_{max}}$$

where q_{max} is the maximum adsorption capacity (mg/g) and K_L is the Langmuir constant (L/mg). The q_{max} and K_L can be determined from the slope and intercept of a linearized plot of C_e/q_e against C_e.

The Freundlich isotherm is written as

$$q_e = K_F C_e^{\,n}$$

where K_F is the adsorption equilibrium constant ((mg/g) (mg/L) $-$ n) and n is a constant indicative of adsorption intensity.

The adsorption isotherms of SMT, NOF, and CTC are shown in Figure 7. For SMT, the Freundlich equation represents a better fit of the experimental data than Langmuir equation (see Table S1 in the Supporting Information). The maximal adsorption capacity calculated by Freundlich model of SMT on CMNPs is increased with the graphitization degree of adsorbents. The Langmuir constant (K_L) of SMT enhances from 124 to 1005 L/mg as untreated CMNPs and CMNPs heated at 200−500 °C are used as adsorbent. Sharp increase of this value is observed on CMNPs (600), CMNPs (700) and CMNPs (850) (7572−23148 L/mg). The trend of the adsorption ability of SMT is consistent with that of the SPE efficiency on CMNPs. Then we conclude that the low recoveries of SMT on untreated CMNPs and CMNPs prepared at 200−500 °C result from its poor adsorption ability on these materials.

The adsorption isotherms of NOF can be described better by Freundlich equation than Langmuir model; while the Langmuir equation is more suitable to fit CTC adsorption than Freundlich equation (see Tables S2 and S3 in the Supporting Information). Adsorption abilities of NOF and CTC on CMNPs adsorbents generally follow the order of CMNPs prepared at 300−500 °C < untreated CMNPs and CMNPs (200) < CMNPs obtained at 600−850 °C. The Langmuir constants of CTC on all CMNPs adsorbents are about 14−170 and 2−35 times higher than those of SMT and NOF, respectively. The adsorption of these highly water-soluble antibiotics on CMNPs should be dominantly controlled by their $\pi-\pi$ stacking interaction with graphitic carbon. The number of benzoic rings, π-bonds or lone pairs of electrons in molecules of these compounds is in the order of CTC > NOF > SMT. Therefore, the adsorption capacity of CTC and NOF are much stronger than that of SMT on all the CMNPs. The quantitative recoveries of CTC on CMNPs prepared at 300−500 °C and NOF on untreated CMNPs and CMNPs prepared at 200−500 °C can be explained by their high adsorption ability to these adsorbents. On the other hand, there are multiple functional groups in the molecule of CTC and NOF (such as −OH, C═O, and CO−NH_2 groups in CTC, and −COOH, −F in NOF). These groups tend to form hydrogen bonds with untreated CMNPs and CMNPs (200) containing more than 36% −COO groups on surface, which is the possible reason for higher adsorption ability of CTC and NOF on untreated CMNPs and CMNPs (200) than that on CMNPs prepared at 300−500 °C. The low recoveries of CTC on untreated CMNPs and CMNPs (200) in Figure 6a may suggest that the formed hydrogen bonds between CTC and adsorbent surface are very strong and hard to desorb.

The SPE trials and batch experiments of antibiotics show that CMNPs prepared at 600−850 °C exhibit great adsorption affinity to most targets contributing to their high graphitization degree of carbon shell. Combined with their large surface areas and recoverability from water due to the strong magnetism of inner core, CMNPs (600), CMNPs (700) and CMNPs (850) have the potential to remove organic pollutants from water samples. However, they are not optimal candidates as SPE adsorbents in most cases because of the hard desorption of adsorbed targets from their surface. In this study, moderate amounts of hydrophilic oxygen-containing groups on CMNPs surface are necessary for quantitative extraction of targets. The abundant O-containing groups on untreated CMNPs and CMNPs (200) are even an advantage for the efficient SPE of quinolones antibiotics.

CONCLUSIONS

Herein, we have developed a simple method to synthesize core/shell structured carbon-encapsulated magnetic nanoparticles (CMNPs). The obtained CMNPs have large surface areas and strong magnetism. The carbon shell is composed of graphitic carbon and diverse oxygen-containing species. Their ratios on carbon shell determine the surface property of CMNPs and are tunable simply by changing the heat treatment temperature in the synthesis process. Combined with perfect adsorption ability of carbon shell and magnetic property of inner core, the nanoscaled CMNPs can quickly and efficiently preconcentrate trace level of organic contaminants from large volume of aqueous solutions based on magnetic SPE technique. The target analytes with weak, medium or high polarity display different retention behaviors on CMNPs adsorbents prepared at low (200 °C), moderate (300−500 °C), and high (600−850 °C) temperature, respectively. Therefore, we anticipate that organic contaminants with a wide range of polarity may be extracted selectively and conveniently from water samples by using these surface-tunable CMNPs adsorbents.

ASSOCIATED CONTENT

Supporting Information

Tables for calculated Langmuir and Freundlich isotherms parameters for antibiotics adsorption on CMNPs. This material is available free of charge via the Internet at http://pubs.acs.org/.

AUTHOR INFORMATION

Corresponding Author

*E-mail: caiyaqi@rcees.ac.cn. Tel: (086) 010-62849182. Fax: (086) 010-62849239.

ACKNOWLEDGMENTS

This work was jointly supported by National Basic Research Program of China (2011CB936001); National Natural Science Foundation of China (20837003, 20907061, 20975110, 20890111).

REFERENCES

(1) Ravelo-Pérez, L. M.; Herrera-Herrera, A. V.; Hernández-Borges, J.; Rodríguez-Delgado, M. A. *J. Chromatogr., A* **2010**, *1217*, 2618−2641.

(2) Šafaříková, M.; Šafařík, I. *J. Magn. Magn. Mater.* **1999**, *194*, 108−102.

(3) Lin, J. H.; Wu, Z. H.; Tseng, W. L. *Anal. Methods* **2010**, *2*, 1874−1879.

(4) Zhao, X. L.; Shi, Y. L.; Wang, T.; Cai, Y. Q.; Jiang, G. B. *J. Chromatogr., A* **2008**, *1188*, 140−147.
(5) Huang, C. Z.; Hu, B. *Spectrochim. Acta, Part B* **2008**, *63*, 437−444.
(6) Zhang, X. L.; Niu, H. Y.; Pan, Y. Y.; Shi, Y. L.; Cai, Y. Q. *Anal. Chem.* **2010**, *82*, 2363−2371.
(7) Zhang, S. X.; Niu, H. Y.; Cai, Y. Q.; Shi, Y. L. *Anal. Chim. Acta* **2010**, *665*, 167−175.
(8) Li, Q. L.; Lam, M. H. W.; Wu, R. S. S.; Jiang, B. W. *J. Chromatogr., A* **2010**, *1217*, 1219−1226.
(9) Gao, Q.; Luo, D.; Ding, J.; Feng, Y. Q. *J. Chromatogr., A* **2010**, *1217*, 5602−5609.
(10) Ding, J.; Gao, Q.; Luo, D.; Shi, Z. G.; Feng, Y. Q. *J. Chromatogr., A* **2010**, *1217*, 7351−7358.
(11) Zhao, X. L.; Shi, Y. L.; Cai, Y. Q.; Mou, S. F. *Environ. Sci. Technol.* **2008**, *1139*, 178−184.
(12) Li, J. D.; Zhao, X. L.; Shi, Y. L.; Cai, Y. Q.; Mou, S. F.; Jiang, G. B. *J. Chromatogr., A* **2008**, *1180*, 24−31.
(13) Ballesteros-Gomez, A.; Rubio, S. *Anal. Chem.* **2009**, *81*, 9012−9020.
(14) Valcárcel, M.; Cárdenas, S.; Simonet, B. M.; Moliner-Martínez, Y.; Lucena, R. *Trends Anal. Chem.* **2008**, *27*, 34−43.
(15) Pyrzyńska, K.; Bystrzejewski, M. *Colloids Surf., A* **2010**, *362*, 102−109.
(16) Park, J. B.; Jeong, S. H.; Jeong, M. S.; Kim, J. Y.; Cho, B. K. *Carbon* **2008**, *46*, 1369−1377.
(17) Byeon, J. H.; Kim, J. W. *ACS Appl. Mater. Interfaces* **2010**, *2*, 947−951.
(18) Bystrzejewski, M.; Karoly, Z.; Szepvolgyi, J.; Kaszuwara, W.; Huczko, A. H. *Carbon* **2009**, *47*, 2040−2048.
(19) Jacob, D. S.; Genish, I.; Klein, L.; Gedanken, A. *J. Phys. Chem. B* **2006**, *110*, 17711−17714.
(20) Wang, J. N.; Zhang, L.; Yu, F.; Sheng, Z. M. *J. Phys. Chem. B* **2007**, *111*, 2119−2124.
(21) Wu, W.; Zhu, Z.; Liu, Z.; Xie, W.; Zhang, J.; Hu, T. *Carbon* **2003**, *41*, 317−321.
(22) Wang, Z. H.; Zhang, Z. D.; Choi, C. J.; Kim, B. K. *J. Alloys Compd.* **2003**, *361*, 289−293.
(23) Huo, J. P.; Song, H. H.; Chen, X. H. *Carbon* **2004**, *42*, 3177−3182.
(24) Zhao, M.; Song, H. H.; Chen, X. H.; Lian, W. T. *Acta Mater.* **2007**, *55*, 6144−6150.
(25) Huo, J. P.; Song, H. H.; Chen, X. H.; Zhao, S. Q.; Xu, C. M. *Mater. Chem. Phys.* **2007**, *101*, 221−227.
(26) Chen, M. A.; Luo, B.; Song, H. H.; Zhi, L. J. *New Carbon Mater.* **2010**, *25*, 199−204.
(27) Geng, J. F.; Jefferson, D. A.; Johnson, B. F. G. *Chem. Commun.* **2004**, 2442−2443.
(28) Yu, S. H.; Cui, X. J.; Li, L. L.; Li, K.; Yu, B.; Antonietti, M.; Cölfen, H. *Adv. Mater.* **2004**, *16*, 1636−1640.
(29) Wang, Z. F.; Guo, H. S.; Yu, Y. L.; He, N. Y. *J. Magn. Magn. Mater.* **2006**, *302*, 397−400.
(30) Zhang, S. X.; Niu, H. Y.; Hu, Z. J.; Cai, Y. Q.; Shi, Y. L. *J. Chromatogr., A* **2010**, *1217*, 4757−4764.
(31) Bai, L.; Mei, B.; Guo, Q. Z.; Shi, Z. G.; Feng, Y. Q. *J. Chromatogr., A* **2010**, *1217*, 7331−7336.
(32) Sun, X. M.; Li, Y. D. *Angew. Chem., Int. Ed.* **2004**, *43*, 597−601.
(33) Lu, A. H.; Li, W. C.; Salabas, E. L.; Spliethoff, B.; Schüth, F. *Chem. Mater.* **2006**, *18*, 2086−2094.
(34) Dresselhaus, M. S.; Jorio, A.; Souza Filho, A. G.; Saito, R. *Philos. Trans. R. Soc. London, Ser. A* **2010**, *368*, 5355−5377.
(35) Fang, H. T.; Liu, C. G.; Liu, C.; Li, F.; Liu, M.; Cheng, H. M. *Chem. Mater.* **2004**, *16*, 5744−5750.
(36) Niu, H. Y.; Cai, Y. Q.; Shi, Y. L.; Wei, F. S.; Mou, S. F.; Jiang, G. B. *J. Chromatogr., A* **2007**, *1172*, 113−120.
(37) Li, X. L.; Luan, T. G.; Liang, Y.; Wong, M. H.; Lan, C. Y. *J. Environ. Sci.* **2007**, *19*, 657−662.
(38) Gatìdou, G.; Thomaìdìs, N. S.; Stasìnakis, A. S.; Lekkas, T. D. *J. Chromatogr., A* **2007**, *1138*, 32−41.
(39) Cai, Y. Q.; Jiang, G. B.; Liu, J. F.; Zhou, Q. X. *Anal. Chem.* **2003**, *75*, 2517−2521.
(40) Cai, Y. Q.; Jiang, G. B.; Liu, J. F.; Zhou, Q. X. *Anal. Chim. Acta* **2003**, *494*, 149−156.
(41) Pan, B.; Xing, B. S. *Environ. Sci. Technol.* **2008**, *42*, 9005−9013.
(42) Pena, A. L.; Lino, C. M.; Silveira, M. I. N. *J. AOAC Int.* **2003**, *86*, 925−929.
(43) Zorita, S.; Larsson, L.; Mathiasson, L. *J. Sep. Sci.* **2008**, *31*, 3117−3121.